How do thalamocortical interactions shape causal structure among resting state brain networks during aging?

Moumita Das, Vanshika Singh, Arpan Banerjee, Dipanjan Roy

Cognitive Brain Dynamics Lab, National Brain Research Centre, NH 8, Manesar, Gurgaon 122052, India

#Email: arpan@nbrc.ac.in, dipanjan.nbrc@gov.in

Abstract

The human brain undergoes both significant structural and functional changes across the lifespan. It is important to understand the underlying causal relationship of the emerging dynamical changes in functional connectivity with age. On average, functional connectivity within resting-state networks weakens in magnitude while connections between resting-state networks tend to increase with age. Further, few recent studies show that effective connectivity within and between large scale resting-state functional networks changes over the healthy lifespan. Motivated by these findings we move one step forward to investigate the effect of the thalamus in the context of healthy aging. Using directed connectivity and weighted net causal outflow measures on resting-state fMRI data, we examine the age-related changes in both cortical and thalamocortical causal interactions within and between resting-state networks. The three of core neurocognitive networks DMN, SN, CEN networks are identified independently by carrying out ICA as well as spatially matching of hub regions with the important RSNs previously reported in the literature. Thereafter, multivariate GCA was performed to test for

causality index between ROIs with and without the inclusion of left and right thalamus. There are two major findings, firstly, we observe that within network causal connections become progressively weaker with age, however, between network causal connections are getting stronger with age among core neurocognitive networks, primarily a reflection of within and between network resting-state functional connectivity. Secondly, significant modifications were found in causal connections and net causal outflows in the presence of thalamus. Finally, we found that the thalamus plays a crucial role as an exogenous drive in the reorganization of within network causal outflow, while Salience network plays a critical role in mediating between network causal outflow with age among cortical networks. Our findings with the weighted causal outflow measures strengthen the hypothesis that balancing within and between network connectivity is perhaps critical for the preservation of cognitive functions with aging.

Keywords: Aging, Effective Connectivity, Multivariate Granger Causal, Neurocognitive Networks, Salience Network, Thalamus, Weighted Net Causal Outflow.

1.Introduction

In the last decade, there has been an enormous interest in studying the coordinated activity in distributed brain areas when the human being is engaged in internally driven tasks, such as meandering through self-referential thoughts while seemingly at rest or more specifically not engaged in a state of goal directed action/ perception (Raichle, 2009; (Bressler & Menon, 2010) ; (Deco, Jirsa, & McIntosh, 2011)). The large scale neurocognitive networks (Bressler Menon, 2010) that chaperons the activity of resting state has been broadly classified in three distinct sub-networks based on the correlation patterns estimated from BOLD time series signals,

namely, the default mode network (DMN), saliency network (SN), and central executive network (CEN) (Menon 2011) . The DMN comprises posterior cingulate cortex (PCC) and medial prefrontal cortex (MPFC) and is implicated in self-referential mental activities (Buckner, Andrews-Hanna, & Schacter, 2008), (Andrews-Hanna, Reidler, Sepulcre, Poulin, & Buckner, 2010) , (Raichle, 2015)). The CEN, comprises rostral and caudal bilateral middle frontal cortex (MFC), bilateral superior Parietal Cortex (SPC) and implicated in decision making and executive functions (Corbetta & Shulman, 2002); (Fox, Corbetta, Snyder, Vincent, & Raichle, 2006)). The SN, which comprise bilateral anterior insula (AI) and caudal, rostral bilateral anterior cingulate cortices (ACC) is important for detection and mapping of salient inputs and routing these inputs to control areas for mediating cognitive control ((Menon & Uddin, 2010);(Uddin, 2015)).

Interestingly, modification of interconnections within and between DMN, CEN, SN is altered in a large number of psychiatric and neurological disorders, for instance, Alzheimer's disease, Autism Spectrum Disorder (ASD), Attention Deficit Hyperactivity Disorder (ADHD), psychosis and depression (Woodward & Cascio, 2015);(Abi-Dargham & Horga, 2016)). SN, in addition to detecting salient stimuli, plays important role in switching between DMN and CEN in the task condition as well as in resting state ((Devarajan, Levitin, & Menon, 2008)). Thus, it integrates and balances internal mental processes with external stimulus-driven cognitive and affective processes. During the performance of many tasks, correlation among the nodes of SN in tandem with CEN increases while the corresponding correlation among the DMN nodes decreases.

An important caveat to all the resting brain network studies are that they mostly concentrate on cortical nodes, and ignores the crucial thalamocortical interactions. The thalamus, a centrally

located relay station for transmitting information throughout the brain, participates in communication with many associative brain regions and involves global multifunctional pathways. Incorporating 10,449 meta-studies, Hwang, Bertolero, Liu, & D'Esposito, 2017 recently showed that the thalamus is engaged in multiple cognitive functions and is a critical integrative hub for functional brain networks. Cross-sectional studies of normal aging have also reported smaller thalamic volumes in older than younger adults (Cherubini, Péran, Caltagirone, Sabatini, & Spalletta, 2009, Hughes et al., 2012;). However, exactly how normal aging affects the thalamic interconnections with other brain networks and its implication in cognitive changes are not completely understood, and thus warrant further investigation. From a methodological standpoint if thalamus acts as a common source to cortical inputs during both rest and task as proposed by theories such as thalamocortical dysryhtmia ((Llinás, Ribary, Jeanmonod, Kronberg, & Mitra, 1999),(Vanneste, Song, & De Ridder, 2018)), a causality analysis that ignores thalamocortical contribution to brain dynamics is of very limited scope and possibly paint an inaccurate account of underlying complexity. Thus, the primary goal of this article is to re-evaluate the interactions among the RSNs: DMN, SN and CEN by taking into consideration the thalamocortical interactions and as a proof of concept characterize how lifespan sculpts the causal neuro-circuity.

2. Material and Methods

2.1 Participants

25 young and 24 elderly individuals participated in this study after providing the written consent. Young (13 females and 12 males) ranged in age from 18-33 years (mean age = 25.68 years). Old (18 females and 6 males) ranged in age from 39-80 years (mean age=58.1 years). All participants gave written informed consent and the study was performed under the compliance of laws and guidelines approved by the ethics committee of Charité University, Berlin.

2.2 Data Acquisition

RS fMRI as well as corresponding diffusion weighted (dw) MRI data were collected from 49 healthy participants at the Charité University Berlin, Germany (Schirner, Rothmeier, Jirsa, McIntosh, & Ritter, 2015). Each fMRI dataset amounts to 661 time points recorded at TR=2s, i.e. about 22 minutes. In the same session, EEG was also recorded, but we do not use the EEG data for our current analysis. No other controlled task was performed. Resting state BOLD activity was recorded while subjects were asked to stay awake with their eyes closed, using a 3T Siemens Trim Trio scanner and a 12 channel Siemens head coil (voxel size $3mm \times 3mm \times 3mm$). Voxel time courses are averaged inside ROIs defined by the Desikan-Killiany atlas (Desikan et al., 2006) as implemented in FreeSurfer. The empirical BOLD time series signals from Regions of Interest (ROI) used in this paper for net causal flow estimations is generated by using an automated pipeline ((Schirner, Rothmeier, Jirsa, McIntosh, & Ritter, 2015)).

2.3 Data Analysis

2.3.1 rs-fMRI preprocessing

The major pre-processing steps on T1 anatomical images were skull stripping, removal of non-brain tissue, brain mask generation, cortical reconstruction, motion correction, intensity normalization, WM and subcortical segmentation, cortical tessellation generating GM–WM and GM–pia interface surface-triangulations and probabilistic atlas-based cortical and subcortical parcellation. These parcellations, segmentations and masks were then used to guide the probabilistic tractography algorithm to estimate connection strengths (a value in the range 0 to 1) between each pair of areas in the cortical gray matter parcellation. The parcellation used in this study is Desikan–Killiany parcellation (Desikan et al., 2006) which consists of 68 cortical regions of interest (ROIs) with 34 ROIs in each hemisphere and 32 subcortical regions. For our

present analysis along with 68 cortical regions, two thalamic regions, left and right thalamus were selected based on this parcellation. FC matrices generated from each subject's MRI data are averaged element-wise to obtain an averaged FC matrix for younger and elderly cohort.

2.3.2 Selection and extraction of three large-scale resting state networks

To identify RSN activity a spatial Group ICA decomposition was performed for the fMRI data of all subjects using FSL MELODIC ((Beckmann & Smith, 2004)) (MELODIC v4.0; FMRIB Oxford University, UK) with the following parameters: high pass filter cut off: 100 s, MCFLIRT motion correction, BET brain extraction, spatial smoothing, normalization to MNI152, temporal concatenation, dimensionality restriction to 30 output components. ICs that correspond to RSNs were automatically identified by spatial correlation with the 9 out of the 10 well-matched pairs of networks of the 29,671-subject Brain Map activation database as described in (Smith et al., 2009) (excluding the cerebellum network). Subsequently, the three key intrinsic networks were identified by spatially matching with pre-existing templates following widely accepted seven network resting state parcellation proposed by Buckner and colleagues (Buckner, Krienen, Castellanos, Diaz, & Yeo, 2011), each of the cortical regions were classified further down to seven parcellated resting networks. In our subsequent analysis, we considered three resting state networks, namely DMN, SN, CEN (Node details are provided in **Table: 1**). We chose for our study Inferior parietal lobule (IPL), PCC and MOF as they constitute core part of DMN ((Andrews-Hanna et al., 2010);(Dixon et al., 2017)) consistently showed activation during mental rumination and self-related processing, mind wandering. The SN, which comprises the anterior insula and caudal, rostral anterior cingulate cortex , is important for detection of salience events and switching between other large scale networks ((Menon & Uddin, 2010);(Uddin, 2015)). Bilateral Rostral and Caudal middle frontal gyrus, superior parietal lobule

were selected as nodes of CEN. The core DMN regions selected in this work consistently showed anticorrelation with SNs ((Fransson, 2005); (Uddin, Kelly, Biswal, Castellanos, & Milham, 2009);(Dixon et al., 2017))

For within network analysis, we used the extracted time series for each six ROI within each respective network. For between network analysis, we combined time series of six ROIs, using principal component analysis, to create a single representative time series of every network.

2.2.4 Effective Connectivity: Multivariate Granger Causal Analysis

Brain signals of different nodes within and between networks are expected to follow a multivariate probability distribution. For instance, let $\boldsymbol{X_t}, \boldsymbol{Y_t}, \boldsymbol{Z_t}$ be a time series of 3 nodes in a network. If there are joint dependencies between $\boldsymbol{X_t}, \boldsymbol{Y_t}, \boldsymbol{Z_t}$ and if we calculate unconditional granger causality between $\boldsymbol{X}$ and $\boldsymbol{Y}$, spurious causalities may occur due to common dependency on $\boldsymbol{Z}$. Thus, to eliminate the possibility of spurious causalities between two time series Multivariate Granger Causality analysis (GCA) was performed to assess the causal influence between nodes of SN, CEN and DMN based on the methods described in ((Barrett, Barnett, & Seth, 2010)). In MVGC spurious causalities are eliminated by conditioning out the common dependencies. According to MVGC approach, if we wish to test the causality from

$\boldsymbol{Y}$ to $\boldsymbol{X}$, we have to consider the full and reduced regressions of the following form

$$\boldsymbol{X}_t = \sum_{k=1}^{p} A_{xx,k}\ \boldsymbol{X}_{t-k} + \sum_{k=1}^{p} A_{xy,k}\ \boldsymbol{Y}_{t-k} + \sum_{k=1}^{p} A_{xz,k}\ \boldsymbol{Z}_{t-k} + \varepsilon_{x,t} \qquad (1)$$

$$\boldsymbol{X}_t = \sum_{k=1}^{p} A'_{xx,k}\ \boldsymbol{X}_{t-k} + \sum_{k=1}^{p} A'_{xz,k}\ \boldsymbol{Z}_{t-k} + \varepsilon'_{x,t} \qquad (2)$$

In full regression (1), the dependence of X on the past of Y, given its own past and the past of Z is incorporated in the coefficients $A_{xy,k}$. If in particular there is no conditional dependence

of X on the past of Y if all the coefficients associated with Y values is zero. This leads to the reduced regression (2), where past values of Y are omitted. Therefore, the null hypothesis of zero causality is :

$H_0 \ : A_{xy.1} = A_{xy.2} = \ \ldots\ldots\ldots = A_{xy.p} = 0$

vs H_1: $at\ least\ one\ A_{xy.k} \neq 0 \ \ for\ k = 1(1)p$ (3)

The granger causality value quantifies the degree to which the full regression model is a better candidate compared to the reduced regression to model $\boldsymbol{X}_t$. Appropriate measure for the model comparison is the logarithm of the ratio of their likelihood values. The joint likelihood of the var model is $L = \left|\Sigma^{\frac{-(m-p)}{2}}\right|$ (where m = total number of nodes, p = estimated model order). This motivates the definition of conditional G- causality statistic as the appropriate log-likelihood ratio. The conditional G -causality from Y to X is defined by

$$F_{y\to x} = \ln\left|\frac{\Sigma'_{xx}}{\Sigma_{xx}}\right| \quad (4)$$

Where $\mathrm{cov}(\varepsilon_{x,t}) = \Sigma_{xx}$, $\mathrm{cov}(\varepsilon'_{x,t}) = \Sigma'_{xx}$ are the error variances of full model and reduced model respectively.

Multivariate granger causality toolbox (Barnett et al.(2014)) was employed to perform the analysis. For each model order p up to the maximum model order (in our case we set it 20), joint likelihood $L = \left|\Sigma^{\frac{-(m-p)}{2}}\right|$ was calculated. Akaike's information criterion and Bayesian information criterion was calculated using L. The order of the vector autoregressive (VAR) model used for computation of the influence measure was selected using the Bayesian information criterion (BIC). Corresponding VAR model parameters, var model coefficients, and covariance matrices were estimated for the estimated model order. Using the reverse solution of the Yule Walker equations, the autocovariance sequences was calculated. For granger causal estimation, var parameters were calculated for both the full and reduced regressions. Granger causality

value was calculated using (4). Significance was tested using F-test. Since multiple causalities were tested simultaneously, FDR correction was used to adjust for multiple hypotheses.

2.2.5 Network Analysis

We further calculated the weighted net granger causal flow to characterise the causal networks in young and elderly groups. To calculate the weighted net granger causal flow, we selected the significant causal outflow connections between the nodes. Weighted out-degree of a node is defined by sum of the strength (granger causal indexes) of significant causal connections from a node in a network to any other node. Likewise weighted in-degree of a node is sum of the strength of causal inflow connections to a node in the network from any other node. Weighted net causal flow was defined as weighted (Out-In) degree. For example, weighted net granger causal outflow of node X, say Δ_x can be expressed using the following formula:

$\Delta_x = (F_{x\to y} + F_{x\to z}) - (F_{y\to x} + F_{z\to x})$ …… (5), provided all F values are significant. Non-significant F-values should be replaced by zero. Similarly, one can calculate Δ_y , Δ_z .

Though F values are positive, weighted net granger causal values can be positive as well as negative also. Positive Δ for a particular node implies, higher causal influence of that node on the other nodes of that network, furthermore negative Δ signifies, that particular node is causally influenced by other nodes of the network.

To compare the net flow of different nodes between young and old age groups we generated 100 bootstrap samples of granger causality index matrices via nonparametric sampling.

For the purpose of comparison, we constructed the distribution of weighted net causal outflow based on the significant causal connections ($p<0.05$, FDR corrected for multiple comparisons). The distribution of weighted net causal outflow was calculated for different nodes within and between network and Wilcoxon signed rank tests were performed to test the significant differences in the net causal outflows for different age group.

3.0 Results

3.1 Reorganization of causality within intrinsic networks with age

3.1.1 Central Executive Network

In CEN, we extracted time series from six nodes (see **figure 2**), namely lRMFG, rRMFG, lCMFG, rCMFG, lSPL, rSPL. The strength of the causal interaction from the rRMFG to the rCMFG was highest among all causal interactions for both elderly and young groups (**figure 3A, 3D**). In addition, significant causal connections ($p < 0.01$, false discovery rate (FDR) corrected) were found from the lRMFG to the lCMFG, and the lSPL for young individuals (**figure 3D**). On the other hand, for elderly group, significant directed causal connectivity was found from the rRMFG to the lSPL and rSPL (in addition to the rCMFG) (**figure 3A**). In contrast to DMN, visually inspecting greater number of inter hemispheric connections were found in elderly individuals in CEN (**figure 3A**).

To further investigate the network properties, weighted net causal outflow for within CEN nodes were calculated. lRMFG and rRMFG acted as a causal outflow hub for young and elderly individuals respectively. Causal outflows were significantly different for all nodes ($p<0.01$). Except lRMFG and rRMFG, all nodes had negative causal outflow (causal inflow) for young individuals **(figure 4A)**. In old cohorts, other than rRMFG, only lCMFG had small positive outflow. All the remaining nodes had causal inflow in old group.

3.1.2 Salience Network

Next we proceed with analysis of salience network which comprise of six nodes (see **figure 2**), namely lInsula, rInsula, lcACC, rcACC, lrACC, rrACC. For within network analysis, multivariate granger causality analysis revealed a smaller number of significant directed causal influences compared to other two networks. The lInsula influenced the lCACC , and the lRACC in young and elderly groups (**figure 3B, 3E**). Additionally, in young significant causal influences were found from the rInsula to the rCACC and from the lRACC to the lInsula . The rInsula also causally influenced the rCACC in young but not in elderly age group **(figure 3E)**.

Weighted net causal outflow analysis revealed lInsula as a causal outlow hub in the salience network for both groups. Other than that, rInsula had positive causal outflow in both groups. lRACC had positive outflow for young cohorts (**figure 4B**). All other nodes had negative outflow (inflow) for both groups. Causal outflows/inflows were significantly different ($p<0.01$) for all the nodes.

3.1.3 Default Mode Network

We performed multivariate granger causal analysis on the extracted time series for each of the six DMN nodes (see **figure 2**) for both young and elderly individuals to depict the age related alteration in dominant direction of influence ($p < 0.05$, false discovery rate (FDR) corrected).While in the younger group, GCA revealed significant directed causal connectivity from the lMOF to the lIPL, lPCC and rMOF to the rIPL, rPCC, lMOF, and lIPL to rIPL, lMOF as shown in **figure 3F**, in elderly individuals, such causal connections from lMOF to lIPL, and lPCC, and lIPL to rIPL were completely absent (**figure 3C**) suggesting an age related decrease in causal drive within DMN networks. Furthermore, the causal connections between rMOF and rIPL was reversed. Visual inspection revealed more number of inter hemispheric causal connections were present in young group compared to old one.

Next, we estimated weighted net causal outflow or weighted (Out-In) degree in both young and elderly group. For the young cohort, rMOF acted as a causal outflow hub among the nodes in DMN, whereas rIPC acted as same for elderly group (**figure 4C**). Based on the 100 bootstrap samples the distribution of weighted net causal outflow was calculated for each of the 6 nodes in DMN. Causal outflows were significantly different in young compared to old (Mann-Whitney test p value < 0.001).

3.2 Comparison of within network causality in three resting state networks in presence of thalamus in young versus old individuals

To investigate the effect of thalamus in shaping within and between network causality, we included thalamus as an additional node in our analysis. For each of the three resting state networks, for within network analysis, we included the right and the left thalami, as the seventh and the eighth nodes. Since the mechanism of the MVGC changes with the number of nodes, the causal strengths were not directly comparable between two networks having different number of nodes. In other words, it is not meaningful to quantify the difference between causal strengths of the same RSN networks before and after the inclusion of the thalami. Instead of that, we focused our analysis to find out the changes in the pattern of causal connections and net causal outflows.

3.2.1 Central Executive Network

In elderly group all the connections except, rRMFG to lSPL remained significant ($p < 0.05$, false discovery rate (FDR) corrected FDR corrected). The connections from the rrMFG to the lSPL was mediated by the lThal. Some significant causal connections were emerging from both the thalami, from the lthal to the lRMFG, the rRMFG, the lSPL, the rSPL, from the rthal to the

lRMFG, the rSPL, and the lSPL for the elderly groups (**figure 5A**). For young groups, all the connections without thalamus also found significant after inclusion of the thalamus (figure). Additionally, the left thalamus causally influenced the lRMFG, the lCMFG, and the rRMFG (**figure 5D**). Right thalamus influenced the node lRMFG.

Net granger causal outflows were significantly changed after inclusion of thalamus for both the young and elderly groups. Effects of thalamus was greater in the younger individual's net causal values (**figure 6A**). Left thalamus acted as a causal outflow hub for both the groups. But the causal outflow in the left thalamus was higher in young compared to elderly group. Causal outflows were significantly different in both the groups for all the eight nodes ($p<0.01$).

3.3.2 Salience Network

Among three resting state networks, the SN was least affected after inclusion of thalamus. No changes were found in causal structure after inclusion of thalamus in elderly individuals (**figure 5B**). In young individuals, significant causal connections were found from the lThal to the lInsula and from the rThal to the rInsula (**figure 5E**). No significant changes were found in the net causal outflow pattern in both the groups. Left thalamus exhibited positive outflow, higher in the case of old individuals ($p<0.05$). Right thalamus received marginally small negative outflow (inflow) for both groups (**figure 6B**).

3.3.3 Default Mode Network

After inclusion of the thalamus in default mode network, there were restructuring in the causal connectivity pattern found in the elderly individuals. On performing multivariate granger causal analysis on DMN after addition of thalami, some of the earlier significant causal connections disappeared while some thalamo-cortical causal connections emerged as important

connections for both the age groups (**figure 5C, 5F**). Causal connection from rIPL to rMOF continued to be the strongest connection in elderly group as found in the previous section without thalamus (**figure 5C**). Other than that, GCA revealed significant causal connections from the rMOF to the rPCC, from the rThal to the lIPl, from the lIPL to the rThal, from the rThal to the lMOF for the elderly people (**figure 5C**). After the introduction of thalami, some of the connections between the left hemispheric nodes disappeared in elderly. For the young group, the effect of the inclusion of thalamus was more pronounced compared to the elderly individuals (**figure 5F**). Instead of the connection from the lMOF to the lPCC, the connection from the lThal to the lPCC emerged as the strongest one after the inclusion of the thalami (though the lMFC to the lPCC connection also remained significant). In addition to that, other significant connections were from the lMOF to the lIPL, from the lThal to the lMOF, from the lThal to rThal, from the lThal to the rPCC, from the rThal to the lMFC, from the rThal to the rMFC, from the rMFC to the rPCC, and from the rMFC to the rIPC (**figure 5F**) suggesting substantial effect of thalamus in reorganizing within network causality in cortical networks and also revealing the effect is the strongest in the younger group compared to elderly. This could be related to the thalamic decline with aging.

Net granger causal outflows were significantly changed after inclusion of the thalamus for the young individuals. Left thalamus emerged as a causal outflow hub for young group. Patterns in the net causal outflows were unchanged in elderly group (**figure 6C**). rIPL continued to be causal outflow hub for elderly group, even after inclusion of thalamus. Causal outflows were significantly different in both groups ($p<0.01$).

3.2 Reorganization of between network causality with age

For between network analysis, we employed principal component analysis, to combine the time series from each of the resting state networks. We took first principal component of the all nodal time series of a network, as one node consisting of the all information of that particular resting state network and performed multivariate granger causality analysis among three nodes. In between network analysis, salience network exhibited prominent causal influence on both default mode network and central executive network in both groups (**figure 7A and 7B**). Causal strengths were significantly higher in old groups compared to young ($p<0.01$). Other directed connectivity between these three nodes were also significant, with presence of higher causal strength in old compared to young suggesting an increase in between network causality with aging.

Next we estimated the weighted net granger causal outflow in between network nodes. Among the three RSNs, the SN was causal outflow hub in the between network analysis. Causal out-flows were significantly different in young and elderly groups ($p< 0.01$) (**figure 8A**).

We repeated between network analysis, with second principal component of all nodal time series of a network taken as a node. No causal connection was found significant, confirming the fact that, first principal component sufficiently explained all the variabilities present in the time series of three intrinsic networks.

3.4 Comparison of between network effective connectivity in presence of Thalamus in young versus old individuals

Next we investigated between network causality in presence of the thalamus for both groups. Causal connections from the thalamus to all three network nodes, namely the DMN, the SN, and the CEN in both age groups were found significant ($p< 0.05$, false discovery rate (FDR) corrected). Thalamus was also causally driven by CEN and SN for both elderly and young groups (**figure 7C and 7D**).

Weighted net causal outflows were significantly affected after inclusion of thalamus. Now thalamus acts as a causal outflow hub for elderly group. SN received highest causal outflow for young group (**figure 8B**). Unlike the within network results, in between network analysis causal outflows were greater in the elderly group. Among other three networks, the SN had positive outflow and the DMN had negative outflow for both the groups. After inclusion of thalamus, outflows in the CEN changed its direction in old cohorts.

Overall, thalamus had not changed the causal connectivity pattern between three resting state networks. After inclusion of thalamus, the causality dynamics between three resting state networks remained unaltered. However, thalamus received causal influences from SN and CEN, also influenced resting state networks. Considering the net causal outflows, causal outflows for the elderly group was affected with inclusion of the thalamus. The effect of thalamus was dissimilar in between network analysis compared to within network analysis. Effect was higher in elderly group.

3.5 Replication Analysis

We identified a group of 50 young and 50 elderly participants from the publicly available Cambridge Aging Neuroscience dataset (https://camcan-archive.mrc-cbu.cam.ac.uk//dataaccess/) in the age range of 18–80 years who did not differ in mean age, gender distribution, or IQ from Berlin dataset. Using this new dataset for independent verification, we conducted identical functional and effective connectivity analyses as in the original dataset and also analysed those measures by varying parcellation and node numbers in each of the three-core neurocognitive resting state networks of interest.

In the replication analysis using the Harvard Oxford atlas, frontoparietal network areas were chosen as the nodes for CEN. These included bilateral FP, LPFC, IFG, SFG and MFG.

Bilateral SPL and PPC were also included in the CEN network in consensus with existing literature. The younger cohort exhibited greater number of causal interactions than the older group (**figure 9A, 9D**). Significant causal connections ($p<0.05$, false discovery rate (FDR) corrected) emerged from left and right thalami both in the young and old groups. However, the strength of causal connections between thalamus and CEN nodes were greater in the younger cohort (**figure 10A, 10D**)

ACC and bilateral RPFC, AInsula, SMG were defined as the nodes of SN in the Harvard Oxford parcellation. As compared to DMN and CEN, multivariate granger causality analysis in Salience network showed lesser number of directed causal influences. (**figure 9B, 9E**) Moreover, right thalamus causally influenced RPFCL in the younger cohort but not in the older cohort (**figure 10B, 10E**).

For the Default mode network, the nodes selected were MPFC, bilateral aMTG, pMTG, to MTG, AG and PCC. Multivariate Granger Causality was performed from the extracted time series to evaluate within network reorganization in young and old cohort.

In the younger group, GCA revealed extensive causal connections between all the DMN nodes (**figure 9F**). Fewer causal connections were observed within the DMN network in the older cohort (**figure 9C**), suggesting an age-related decrease in causal drive. Presence of causal connections of the DMN nodes with thalamus in the young (**figure 10F**) but not in the old cohort reiterates the notion of thalamic decline with ageing.

In between network analysis, salience network emerged to have the highest causal strength, exhibiting prominent causal influence on DMN and CEN in both young and old cohort. Net causal outflows were significantly different for both age group.

4. Discussion

In the recent past, several studies have endeavoured to unravel the changes in the brain's structural and functional connectivity with aging and their cognitive implications. A vast majority of these studies have used temporal correlation across different brain regions as measure of functional connectivity to characterize ageing related changes in brain's large-scale functional connectivity patterns. In the present study, we employ multi variate granger causality analysis to probe within- and between- network causal relationships among three key intrinsic resting state brain networks with the hope to facilitate more biologically meaningful interpretations with healthy aging. Every cortical region receives feedforward projections from the thalamus and in turn sends outputs to one or multiple thalamic nuclei (Obeso et al.,2008);(McFarland et al.,2002). Thalamocortical projections relay nearly all incoming information to the cortex as well as mediate corticocortical communication (Sherman and Gui). Thus, a fuller insight into brain functional characterization certainly requires knowledge of the organization and properties of thalamocortical interactions. A recent study by ((Hwang, Bertolero, Liu, & D'Esposito, 2017)) showed thalamus as an integrative hub for functional networks. A handful of studies also observed disrupted thalamic resting state functional networks, in brain injury, schizophrenia((Tang et al., 2011);(Wang, Rau, Li, Chen, & Yu, 2015a)). (Goldstone, Mayhew, Hale, Wilson, & Bagshaw, 2018) investigated the association of thalamic functional connectivity with behavioural performance in elderly population. In continuation of earlier works on thalamic functional connectivity, we extend it to thalamic effective connectivity by not concentrating entirely on cortical nodes, and pinpointing how such interactions are driven with age by common exogeneous thalamocortical inputs during endogenous activities.

We investigate the changes in the causal dynamics in RSNs with the inclusion of thalamus in our analysis. Overall, we found significant reconfiguration of between- and within-network

effective connectivity with aging. Our study also reveals the salience network's role as a mediator of switching between DMN and CEN with aging, a finding that is in line with the extant literature ((Menon & Uddin, 2010); (Bonnelle et al., 2012)). Beyond this, we also find that the role of salience network as a mediator is getting even more prominent with aging, leading to reduced segregation and increased integration of resting state networks with aging. Finally, we demonstrate that how thalamus plays a crucial role in restructuring cortical network causality with aging.

According to the dedifferentiation hypothesis of cognitive aging, age-related impairments in cognitive function arise from reduced distinctiveness of neural representations ((Li, Lindenberger, & Sikström, 2001)). Historically, the concept of dedifferentiation was introduced by Baltes and colleagues ((Baltes & et, 1980)) to account for age-related increases in the correlation between levels of performance on different cognitive tasks. At the neural level, numerous brain-imaging studies have shown that the aging brain adapts to the age-related changes by exhibiting more global activation compared to younger individuals while performing a cognitive/motor task ((Cabeza, 2002); (Reuter-Lorenz, 2002);(Serrien, Ivry, & Swinnen, 2007); (Seidler et al., 2010)). In line with these finding, at the network level, several studies have found a decrease in within-network functional connectivity and an increase in between-network functional connectivity in RSNs ((Andrews-Hanna et al., 2007);(Betzel et al., 2014);(Ferreira & Busatto, 2013);(Ferreira et al., 2016);(Geerligs et al., 2015);(Ng, Lo, Lim, Chee, & Zhou, 2016)) with aging. Overall, our study reproduces these results with effective connectivity analysis and find that the reorganization in causal connectivity patterns with age primarily reflects functional connectivity patterns. More specifically, younger individuals show increase in both the number and the strength of causal connections within DMN, CEN, and SN. At the between-network level, we find, using principal component analysis, that causal

strengths are significantly higher in the elderly individuals compared to the young thus further substantiating the dedifferentiation hypothesis. Moreover, the present study also uncovers several novel observations, e.g., the reversal of direction of causal connections between rMOF and rIPL with aging, age-related changes in the causal outflow in key nodes of the RSNs and reconfiguration of causal outflow hubs and so on that are inaccessible to a functional connectivity analysis. Thus, future studies should continue to investigate brain networks across the lifespan employing MVGC and other-directed connectivity measures.

The role of salience network in mediating switching between DMN and CEN is well established ((Sridharan et al., 2008); (Menon & Uddin, 2010); (Goulden et al., 2014)). In agreement with these observations, we find SN to exert strong causal influence on both DMN and CEN in both the age groups. In between network analysis, SN is found to act as a causal outflow hub among three RSNs we investigated. Interestingly, the causal influence of SN on both DMN and CEN increases with aging. An increase in the between network causality in elderly group emerges as a general trend in our analysis, and the above finding may reflect this general trend.

Thalamus has extensive connections with the entire cerebral cortex. By performing graph-theoretic analyses on thalamocortical functional connectivity data, ((Hwang et al., 2017)) demonstrated that thalamus integrates multimodal information across diverse cortical functional networks and act as an integrative hub for functional brain networks. The association between thalamocortical functional connectivity abnormalities and cognitive deficits in clinical conditions like schizophrenia ((Wang, Rau, Li, Chen, & Yu, 2015b),) is already known. Also known is the fact that thalamic volume significantly decreases with aging ((Walhovd et al., 2005);(Cherubini, Péran, Caltagirone, Sabatini, & Spalletta, 2009);(Zheng et al., 2018)). However, only a handful of studies (e.g.(Goldstone et al., 2018)) have investigated the thalamic

influence in reorganizing resting state networks with aging and none has employed the causal analysis. In our analysis with effective connectivity measures thalamus emerges as an important node to critically influence both within- and between- network connectivity patterns among RSNs. After inclusion of thalamus in the between network analysis, thalamus acts as a causal outflow hub and causally drives all three network nodes for both the age groups. In contrast, in within network analysis, the influence of thalamus in reorganizing within network causality is much more prominent in younger age group compared to the elderly. In DMN, Left thalamus comes out as a causal outflow hub for young group while patterns in the net causal outflows were unchanged in elderly group compared to the without thalamus analysis. After inclusion of thalamus in CEN within network analysis, though left thalamus acts as a causal outflow hub for both the groups, the causal outflow values are higher in young compared to elderly group. This preferential influence of thalamus on younger individual is consistent with the thalamic decline with aging as discussed above. Also, among three resting state networks, the SN remains least affected after inclusion of thalamus, both in within- and between- network analysis. No changes were found in causal architecture within SN after inclusion of thalamus in elderly individuals. In young individuals also changes are minimal. The net causal outflow pattern also does not change after inclusion of thalamus in both the groups. These findings are in concurrence with the observations made by the previous studies ((Wang et al., 2015b);(Cao et al., 2014); (Sakaki et al., 2016); (Xiao et al., 2018)) that in contrast to DMN and CEN, within network connectivity is preserved or increased in SN with aging. Our result suggests that this preservation of connectivity within SN may be driven by thalamus.

We have performed our replication analysis, with different cohort and different brain parcellation atlas. Even though, different nodes were used for three RSN, some of the major findings with the earlier dataset were replicated. In within network analysis, greater number of causal connections with higher strengths in younger group compared to old individuals are consistent

with our findings with Berlin data set. Effect of thalamus is also revealed by higher number of causal connections from thalamus to other nodes in younger group compared to old individuals.

We acknowledge several limitations of our study that should be addressed by the future studies. The result should be replicated in a larger lifespan cohort comprise of middle young and middle elderly groups to get additional insights and true estimate of lifespan trend in causal outflow in resting state networks. Future research should also investigate the sensitivity of the analysis to the choice of different brain parcellation schemes.

Finally, thalamus is a heterogenous structure composed of several nuclei; each of which sends distinct afferent inputs to cortical regions as well as driven by cortical outputs (add reference). Thus, probing the influence of different nuclei of thalamus on reorganization of within- and between- network causality of different RSNs would help to better describe the complex neurophysiological processes taking place in the brain with aging. In general, the analysis could be extended to other subcortical regions to understand how cortical-subcortical connectivity impact the cognitive ability across age.

In conclusion, the results of the present study demonstrate that effective connectivity analysis can provide crucial insights regarding within- and between- network information flow across lifespan over and above insights provided by functional connectivity measures. This study also establishes thalamus as a common driver of organization and reorganization of RSNs with aging, a conclusion that should encourage future research to explore the influences exerted by subcortical structures on cortical networks and their clinical implications.

Acknowledgement

This study was supported by NBRC Core funds, Ramalingaswami Fellowships (Department of Biotechnology, Government of India) to DR (BT/RLF/Re-entry/07/2014) and AB (BT/RLF/Re601entry/31/2011) and Innovative Young Biotechnologist Award (IYBA) to AB (BT/07/IYBA/2013).AB also acknowledges the support of the Centre of Excellence in Epilepsy and MEG. DR was also supported by SR/CSRI/21/2016 extramural grant from the Department of Science and Technology (DST) Ministry of Science and Technology, Government of India. Data collection and sharing for this project was provided by the Cambridge Centre for Ageing and Neuroscience (CamCAN). CamCAN funding was provided by the UK Biotechnology and Biological Sciences Research Council (grant number BB/H008217/1), together with support from the UK Medical Research Council and University of Cambridge, UK.

References

Abi-Dargham, A., & Horga, G. (2016). The search for imaging biomarkers in psychiatric disorders. *Nature Medicine*, *22*(11), 1248–1255. https://doi.org/10.1038/nm.4190

Andrews-Hanna, J. R., Reidler, J. S., Sepulcre, J., Poulin, R., & Buckner, R. L. (2010). Functional-Anatomic Fractionation of the Brain's Default Network. *Neuron*, *65*(4), 550–562. https://doi.org/10.1016/j.neuron.2010.02.005

Andrews-Hanna, J. R., Snyder, A. Z., Vincent, J. L., Lustig, C., Head, D., Raichle, M. E., & Buckner, R. L. (2007). Disruption of large-scale brain systems in advanced aging. *Neuron*, *56*(5), 924–935. https://doi.org/10.1016/j.neuron.2007.10.038

Baltes, P. B., & et, al. (1980). Integration versus differentiation of fluid/crytallized intelligence in old age. *Developmental Psychology*, *16*(6), 625–635. https://doi.org/10.1037/0012-1649.16.6.625

Barrett, A. B., Barnett, L., & Seth, A. K. (2010). Multivariate Granger causality and generalized variance. *Physical Review E - Statistical, Nonlinear, and Soft Matter Physics*, *81*(4). https://doi.org/10.1103/PhysRevE.81.041907

Beckmann, C. F., & Smith, S. M. (2004). Probabilistic Independent Component Analysis for

Functional Magnetic Resonance Imaging. *IEEE Transactions on Medical Imaging*, *23*(2), 137–152. https://doi.org/10.1109/TMI.2003.822821

Betzel, R. F., Byrge, L., He, Y., Goñi, J., Zuo, X. N., & Sporns, O. (2014). Changes in structural and functional connectivity among resting-state networks across the human lifespan. *NeuroImage*, *102*(P2), 345–357. https://doi.org/10.1016/j.neuroimage.2014.07.067

Bonnelle, V., Ham, T. E., Leech, R., Kinnunen, K. M., Mehta, M. A., Greenwood, R. J., & Sharp, D. J. (2012). Salience network integrity predicts default mode network function after traumatic brain injury. *Proceedings of the National Academy of Sciences*, *109*(12), 4690–4695. https://doi.org/10.1073/pnas.1113455109

Bressler, S. L., & Menon, V. (2010, June). Large-scale brain networks in cognition: emerging methods and principles. *Trends in Cognitive Sciences*, Vol. 14, pp. 277–290. https://doi.org/10.1016/j.tics.2010.04.004

Buckner, R. L., Andrews-Hanna, J. R., & Schacter, D. L. (2008). The brain's default network: Anatomy, function, and relevance to disease. *Annals of the New York Academy of Sciences*, *1124*, 1–38. https://doi.org/10.1196/annals.1440.011

Buckner, R. L., Krienen, F. M., Castellanos, A., Diaz, J. C., & Yeo, B. T. T. (2011). The organization of the human cerebellum estimated by intrinsic functional connectivity. *Journal of Neurophysiology*, *106*(5), 2322–2345. https://doi.org/10.1152/jn.00339.2011

Cabeza, R. (2002). Hemispheric asymmetry reduction in older adults: The HAROLD model. *Psychology and Aging*, *17*(1), 85–100. https://doi.org/10.1037/0882-7974.17.1.85

Cao, W., Luo, C., Zhu, B., Zhang, D., Dong, L., Gong, J., … Yao, D. (2014). Resting-state functional connectivity in anterior cingulate cortex in normal aging. *Frontiers in Aging Neuroscience*, *6*, 280. https://doi.org/10.3389/fnagi.2014.00280

Cherubini, A., Péran, P., Caltagirone, C., Sabatini, U., & Spalletta, G. (2009). Aging of

subcortical nuclei: Microstructural, mineralization and atrophy modifications measured in vivo using MRI. *NeuroImage*, *48*(1), 29–36. https://doi.org/10.1016/j.neuroimage.2009.06.035

Corbetta, M., & Shulman, G. L. (2002). Control of goal-directed and stimulus-driven attention in the brain. *Nature Reviews Neuroscience*, *3*(3), 201–215. https://doi.org/10.1038/nrn755

Deco, G., Jirsa, V. K., & McIntosh, A. R. (2011). Emerging concepts for the dynamical organization of resting-state activity in the brain. *Nature Reviews. Neuroscience*, *12*(1), 43–56. https://doi.org/10.1038/nrn2961

Desikan, R. S., Ségonne, F., Fischl, B., Quinn, B. T., Dickerson, B. C., Blacker, D., … Killiany, R. J. (2006). An automated labeling system for subdividing the human cerebral cortex on MRI scans into gyral based regions of interest. *NeuroImage*, *31*(3), 968–980. https://doi.org/10.1016/j.neuroimage.2006.01.021

Dixon, M. L., Andrews-Hanna, J. R., Spreng, R. N., Irving, Z. C., Mills, C., Girn, M., & Christoff, K. (2017). Interactions between the default network and dorsal attention network vary across default subsystems, time, and cognitive states. *NeuroImage*, *147*, 632–649. https://doi.org/10.1016/j.neuroimage.2016.12.073

Ferreira, L. K., & Busatto, G. F. (2013). Resting-state functional connectivity in normal brain aging. *Neuroscience and Biobehavioral Reviews*, *37*(3), 384–400. https://doi.org/10.1016/j.neubiorev.2013.01.017

Ferreira, L. K., Regina, A. C. B., Kovacevic, N., Martin, M. D. G. M., Santos, P. P., Carneiro, C. D. G., … Busatto, G. F. (2016). Aging effects on whole-brain functional connectivity in adults free of cognitive and psychiatric disorders. *Cerebral Cortex*, *26*(9), 3851–3865. https://doi.org/10.1093/cercor/bhv190

Fox, M. D., Corbetta, M., Snyder, A. Z., Vincent, J. L., & Raichle, M. E. (2006).

Spontaneous neuronal activity distinguishes human dorsal and ventral attention systems. *Proceedings of the National Academy of Sciences of the United States of America*, *103*(26), 10046–10051. https://doi.org/10.1073/pnas.0604187103

Fransson, P. (2005). Spontaneous low-frequency BOLD signal fluctuations: An fMRI investigation of the resting-state default mode of brain function hypothesis. *Human Brain Mapping*, *26*(1), 15–29. https://doi.org/10.1002/hbm.20113

Geerligs, L., Rubinov, M., Tyler, L. K., Brayne, C., Bullmore, E. T., Calder, A. C., … Henson, R. N. (2015). State and trait components of functional connectivity: Individual differences vary with mental state. *Journal of Neuroscience*, *35*(41), 13949–13961. https://doi.org/10.1523/JNEUROSCI.1324-15.2015

Goldstone, A., Mayhew, S. D., Hale, J. R., Wilson, R. S., & Bagshaw, A. P. (2018). Thalamic functional connectivity and its association with behavioral performance in older age. *Brain and Behavior*, *8*(4). https://doi.org/10.1002/brb3.943

Goulden, N., Khusnulina, A., Davis, N. J., Bracewell, R. M., Bokde, A. L., McNulty, J. P., & Mullins, P. G. (2014). The salience network is responsible for switching between the default mode network and the central executive network: replication from DCM. *NeuroImage*, *99*, 180–190. https://doi.org/10.1016/j.neuroimage.2014.05.052

Hwang, K., Bertolero, M. A., Liu, W. B., & D'Esposito, M. (2017). The Human Thalamus Is an Integrative Hub for Functional Brain Networks. *The Journal of Neuroscience*, *37*(23), 5594–5607. https://doi.org/10.1523/jneurosci.0067-17.2017

Li, S. C., Lindenberger, U., & Sikström, S. (2001, November 1). Aging cognition: From neuromodulation to representation. *Trends in Cognitive Sciences*, Vol. 5, pp. 479–486. https://doi.org/10.1016/S1364-6613(00)01769-1

Llinás, R. R., Ribary, U., Jeanmonod, D., Kronberg, E., & Mitra, P. P. (1999). Thalamocortical dysrhythmia: A neurological and neuropsychiatric syndrome

characterized by magnetoencephalography. *Proceedings of the National Academy of Sciences of the United States of America*, *96*(26), 15222–15227. https://doi.org/10.1073/pnas.96.26.15222

McFarland, N. R., & Haber, S. N. (2002). Thalamic relay nuclei of the basal ganglia form both reciprocal and nonreciprocal cortical connections, linking multiple frontal cortical areas. *Journal of Neuroscience*, *22*(18), 8117-8132.

Menon, V., & Uddin, L. Q. (2010). Saliency, switching, attention and control: a network model of insula function. *Brain Structure & Function*, Vol. 214, pp. 655–667. https://doi.org/10.1007/s00429-010-0262-0

Ng, K. K., Lo, J. C., Lim, J. K. W., Chee, M. W. L., & Zhou, J. (2016). Reduced functional segregation between the default mode network and the executive control network in healthy older adults: A longitudinal study. *NeuroImage*, *133*, 321–330. https://doi.org/10.1016/j.neuroimage.2016.03.029

Obeso, J. A., Rodríguez-Oroz, M. C., Benitez-Temino, B., Blesa, F. J., Guridi, J., Marin, C., & Rodriguez, M. (2008). Functional organization of the basal ganglia: therapeutic implications for Parkinson's disease. *Movement disorders: official journal of the Movement Disorder Society*, *23*(S3), S548-S559.

Raichle, M. E. (2015). The Brain’s Default Mode Network. *Annual Review of Neuroscience*, *38*(1), 433–447. https://doi.org/10.1146/annurev-neuro-071013-014030

Reuter-Lorenz, P. A. (2002). New visions of the aging mind and brain für mehr Artikel. *Trends in Cognitive Sciences*, *6*(9), 394–400. https://doi.org/10.1016/S1364-6613(02)01957-5

Sakaki, M., Yoo, H. J., Nga, L., Lee, T. H., Thayer, J. F., & Mather, M. (2016). Heart rate variability is associated with amygdala functional connectivity with MPFC across

younger and older adults. *NeuroImage*, *139*, 44–52. https://doi.org/10.1016/j.neuroimage.2016.05.076

Schirner, M., Rothmeier, S., Jirsa, V. K., McIntosh, A. R., & Ritter, P. (2015). An automated pipeline for constructing personalized virtual brains from multimodal neuroimaging data. *NeuroImage*, *117*, 343–357. https://doi.org/10.1016/j.neuroimage.2015.03.055

Seidler, R. D., Bernard, J. A., Burutolu, T. B., Fling, B. W., Gordon, M. T., Gwin, J. T., … Lipps, D. B. (2010). Motor control and aging: links to age-related brain structural, functional, and biochemical effects. *Neuroscience and Biobehavioral Reviews*, *34*(5), 721–733. https://doi.org/10.1016/j.neubiorev.2009.10.005

Serrien, D. J., Ivry, R. B., & Swinnen, S. P. (2007). The missing link between action and cognition. *Progress in Neurobiology*, *82*(2), 95–107. https://doi.org/10.1016/j.pneurobio.2007.02.003

Smith, S. M., Fox, P. T., Miller, K. L., Glahn, D. C., Fox, P. M., Mackay, C. E., … Beckmann, C. F. (2009). Correspondence of the brain's functional architecture during activation and rest. *Proceedings of the National Academy of Sciences of the United States of America*, *106*(31), 13040–13045. https://doi.org/10.1073/pnas.0905267106

Sridharan, D., Levitin, D. J., & Menon, V. (2008). A critical role for the right fronto-insular cortex in switching between central-executive and default-mode networks. *Proceedings of the National Academy of Sciences of the United States of America*, *105*(34), 12569–12574. https://doi.org/10.1073/pnas.0800005105

Tang, L., Ge, Y., Sodickson, D. K., Miles, L., Zhou, Y., Reaume, J., & Grossman, R. I. (2011). Thalamic resting-state functional networks: Disruption in patients with mild traumatic brain injury. *Radiology*, *260*(3), 831–840. https://doi.org/10.1148/radiol.11110014

Uddin, L. Q. (2015). Salience processing and insular cortical function and dysfunction.

Nature Reviews Neuroscience, *16*(1), 55–61. https://doi.org/10.1038/nrn3857

Uddin, L. Q., Kelly, A. M. C., Biswal, B. B., Castellanos, F. X., & Milham, M. P. (2009). Functional Connectivity of Default Mode Network Components: Correlation, Anticorrelation, and Causality. *Human Brain Mapping*, *30*(2), 625–637. https://doi.org/10.1002/hbm.20531

Vanneste, S., Song, J. J., & De Ridder, D. (2018). Thalamocortical dysrhythmia detected by machine learning. *Nature Communications*, *9*(1). https://doi.org/10.1038/s41467-018-02820-0

Walhovd, K. B., Fjell, A. M., Reinvang, I., Lundervold, A., Dale, A. M., Eilertsen, D. E., … Fischl, B. (2005). Effects of age on volumes of cortex, white matter and subcortical structures. *Neurobiology of Aging*, *26*(9), 1261–1270; discussion 1275-8. https://doi.org/10.1016/j.neurobiolaging.2005.05.020

Wang, H. L. S., Rau, C. L., Li, Y. M., Chen, Y. P., & Yu, R. (2015a). Disrupted thalamic resting-state functional networks in schizophrenia. *Frontiers in Behavioral Neuroscience*, *9*(FEB), 1–9. https://doi.org/10.3389/fnbeh.2015.00045

Wang, H. L. S., Rau, C. L., Li, Y. M., Chen, Y. P., & Yu, R. (2015b). Disrupted thalamic resting-state functional networks in schizophrenia. *Frontiers in Behavioral Neuroscience*, *9*(FEB). https://doi.org/10.3389/fnbeh.2015.00045

Woodward, N. D., & Cascio, C. J. (2015). Resting-State Functional Connectivity in Psychiatric Disorders. *JAMA Psychiatry*, *72*(8), 743–744. https://doi.org/10.1001/jamapsychiatry.2015.0484

Xiao, T., Zhang, S., Lee, L. E., Chao, H. H., van Dyck, C., & Li, C. S. R. (2018). Exploring age-related changes in resting state functional connectivity of the Amygdala: From young to middle adulthood. *Frontiers in Aging Neuroscience*, *10*(JUL). https://doi.org/10.3389/fnagi.2018.00209

Zheng, F., Cui, D., Zhang, L., Zhang, S., Zhao, Y., Liu, X., … Qiu, J. (2018). The volume of hippocampal subfields in relation to decline of memory recall across the adult lifespan. *Frontiers in Aging Neuroscience*, *10*(OCT). https://doi.org/10.3389/fnagi.2018.00320

Table 1

Coordinates of selected nodes of three resting state networks according to Desikan-Killiany parcellation atlas

Network	Region	MNI coordinates (x,y,z)	
		Left (l)	Right(r)
Salience Network	Insula (Insula)	(-41, 13, -6)	(43,12,-6)
	Caudal anterior cingulate cortex (CACC)	(-2,21,27)	(3, 21, 27)
	Rostral anterior cingulate cortex (RACC)	(-2,39,6)	(4, 38,4)
Central Executive Network	Rostral middle frontal gyrus (RMFG)	(-34, 53, 17)	(43, 45, 21)
	Caudal middle frontal gyrus (CMFG)	(-45, 18, 46)	(43, 14, 43)
	Superior parietal lobule (SPL)	(-25, -62, 63)	(17,-65,59)
Default Mode Network	Medial orbitofrontal (MOF)	(-4, 44, -14)	(7, 45, -13)
	Inferior parietal lobule (IPL)	(-47, -70, 31)	(48, -67,29)
	Posterior cingulate cortex (PCC)	(-1, -18, 38)	(1, -16, 37)

Figure 1. Flow chart describing major steps employed in our pipeline for estimation of causal connectivity and weighted outflow analysis using MVGC

Figure 2. ROIs selected based on seven networks resting state parcellation proposed by Yeo et al. (2011) (cite). The ROIs (circles) related 3 prominent brain networks are overlaid on the spatial distribution maps derived from group ICA of multiple resting state networks of interest that is, the default mode network ROIs (DMN), the salience network ROIs (SN), and the Control network or Central Executive Network (CEN)

Figure 3. Effective Connectivity between the nodes of three resting state networks. Effective connectivity between **A.** six key nodes of CEN (green), **B.** six key nodes of SN (yellow), **C.** six key nodes of DMN (red) for elderly group. **D.** six key nodes of CEN (green), **E.** six key nodes of SN (yellow), **F.** six key nodes of DMN (red) for young group.

Figure 4. Weighted net causal flow for within network effective connectivity analysis. A. Weighted net causal outflow in nodes of the central executive network **B.** Weighted Net causal outflow in nodes of the salience network **C.** Weighted net causal outflow in nodes of default mode network. Weighted net causal outflows were significantly different in few nodes in each of the three RSN young and elderly group ($p < 0.05$ is indicated by '*', $p<0.01$ is indicated by '**', No significant difference is indicated by 'NS')

Figure 5. Effective Connectivity between the nodes of three resting state networks and the thalamus. **A.** Effective connectivity between six key nodes of CEN (green), **B.** six key nodes of SN (yellow), **C.** six key nodes of DMN (red) for elderly group in presence of thalamic

nodes (blue). **D.** Effective connectivity between six key nodes of CEN (green), **E.** six key nodes of SN (yellow), **F.** six key nodes of DMN (red) for elderly group in presence of thalamic nodes (blue) for young group in presence of thalamic nodes (blue).

Figure 6. Weighted net causal outflow for within network effective connectivity analysis **A.** Weighted net causal outflow in nodes of the central executive network and two thalamic regions (left, right). **B.** Weighted net causal outflow in nodes of the salience network and two thalamic regions (left,right). **C.** Weighted Net causal outflow for default mode network and two thalamic regions (left, right). Weighted net causal outflows were significantly different in few nodes in each of the three RSN young and elderly group ($p < 0.05$ is indicated by '*', $p<0.01$ is indicated by '**', No significant difference is indicated by 'NS') .

Figure 7. Effective connectivity between three resting state networks in absence and presence of the thalamus. **A.** Effective connectivity between three nodes representing three RSN, SN (yellow), DMN (red), CEN (green) for old population. **B.** Results for Effective connectivity between three nodes representing three RSN for young population **C.** Effective connectivity between three nodes representing three RSN and fourth node representing the thalamus (blue) for old population **D.** Effective connectivity between three nodes representing three RSN and fourth node representing the thalamus for young population

Figure 8. Weighted net causal outflow for between network effective connectivity analysis A. Weighted net causal outflow in three RSN **B.** Weighted net causal outflow in three RSN and the thalamus. Weighted net causal outflows were significantly different in few nodes in each of the three RSN young and elderly group ($p<0.01$ is indicated by '**', No significant difference is indicated by 'NS') .

Figure 9. Effective Connectivity between the nodes of three resting state networks using Harvard Oxford Atlas. Effective connectivity between **A.** key nodes of CEN (green), **B.** key nodes of SN (yellow), **C.** key nodes of DMN (red) for elderly group. **D.** key nodes of CEN (green), **E.** key nodes of SN (yellow), **F.** key nodes of DMN (red) for young group.

Figure 10. Effective Connectivity between the nodes of three resting state networks and the thalamus using Harvard Oxford Atlas. Effective connectivity between **A**. key nodes of CEN (green), **B**. key nodes of SN (yellow), **C.** key nodes of DMN (red) for elderly group in presence of thalamic nodes (blue). **D.** Effective connectivity between key nodes of CEN (green), **E.** key nodes of SN (yellow), **f.** key nodes of DMN (red) for young group in presence of thalamic nodes (blue).

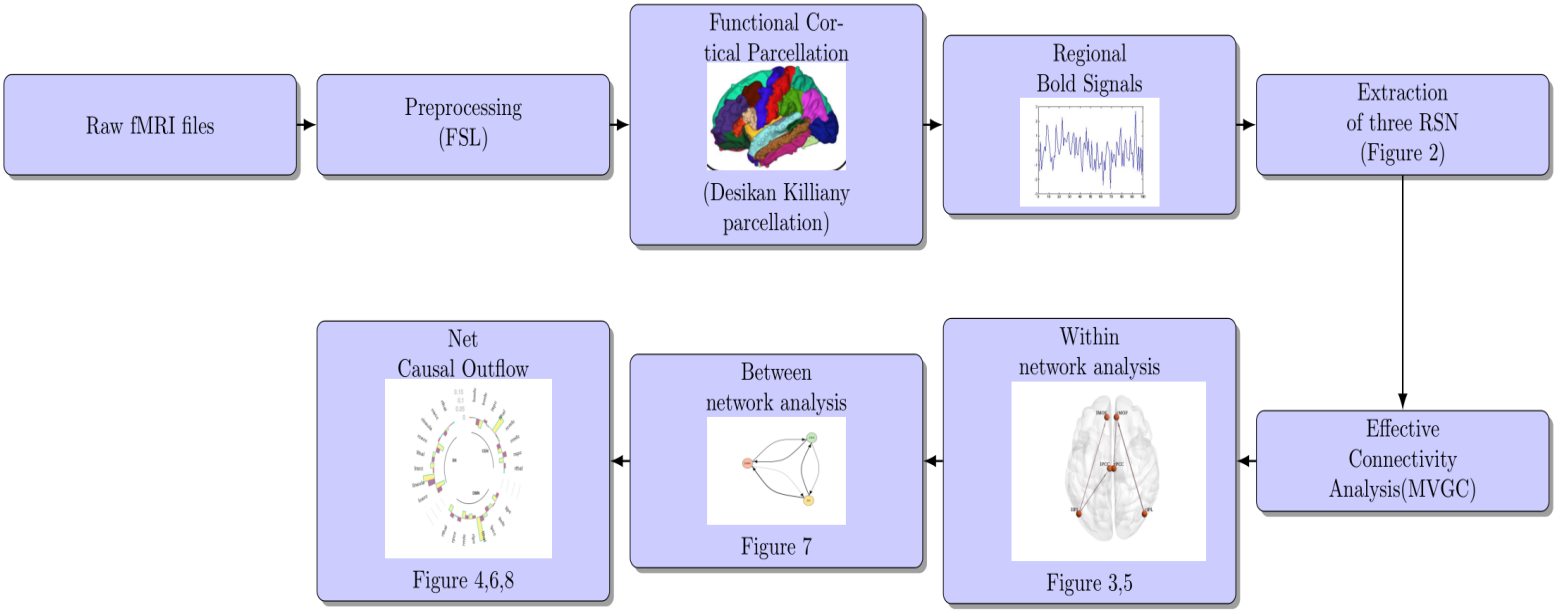
Raw fMRI files
Preprocessing
(FSL)
Functional Cor-
tical Parcellation
(Desikan Killiany
parcellation)
Regional
Bold Signals
Extraction
of three RSN
(Figure 2)
Effective
Connectivity
Analysis(MVGC)
Within
network analysis
Figure 3,5
Between
network analysis
Figure 7
Net
Causal Outflow
Figure 4,6,8

Figure 1.

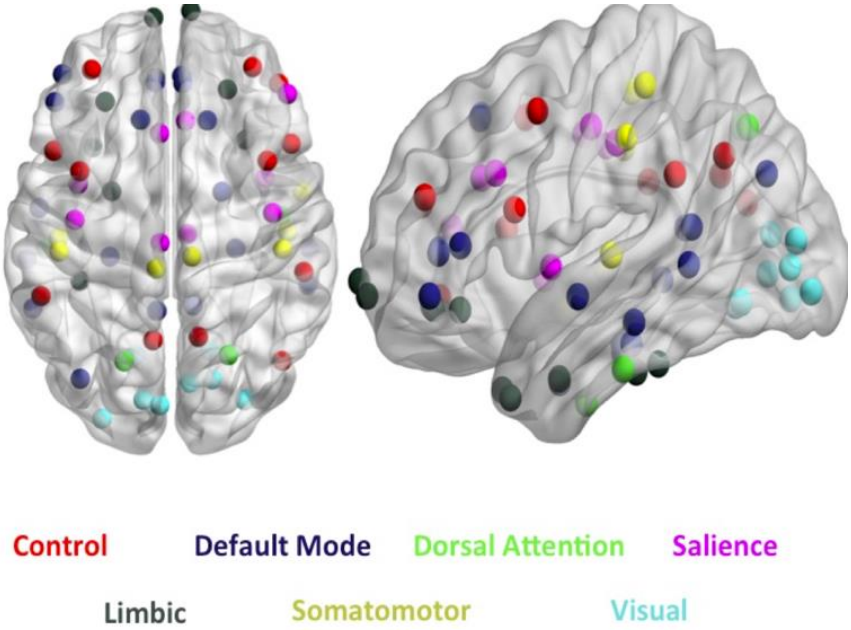
Control
Default Mode
Dorsal Attention
Salience
Limbic
Somatomotor
Visual

Figure 2.

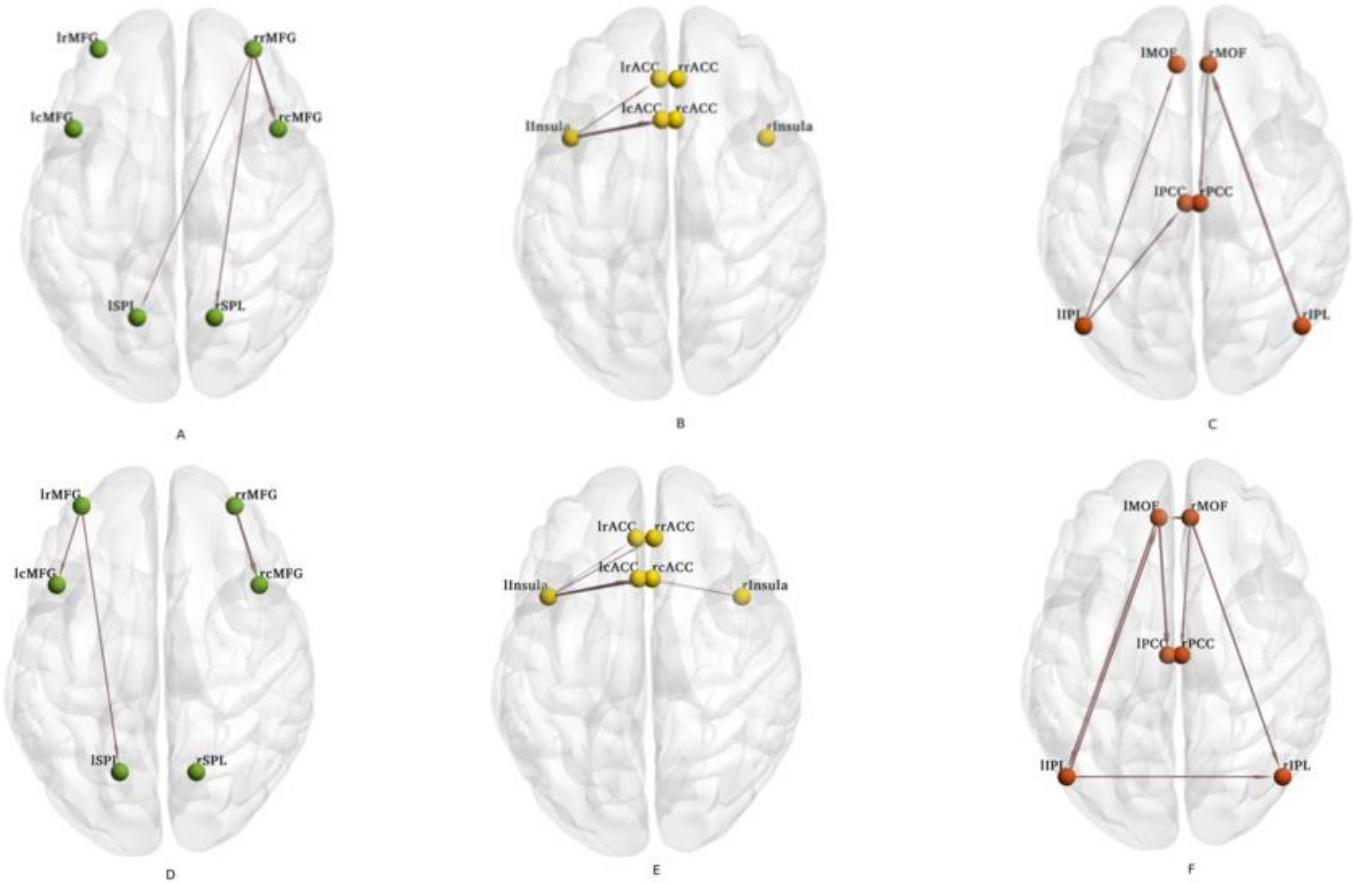
lrMFG
rrMFG
lcMFG
rcMFG
lSPL
rSPL
A
lrACC
rrACC
lcACC
rcACC
lInsula
rInsula
B
lMOF
rMOF
lPCC
rPCC
lIPL
rIPL
C
lrMFG
rrMFG
lcMFG
rcMFG
lSPL
rSPL
D
lrACC
rrACC
lcACC
rcACC
lInsula
rInsula
E
lMOF
rMOF
lPCC
rPCC
lIPL
rIPL
F

Figure 3.

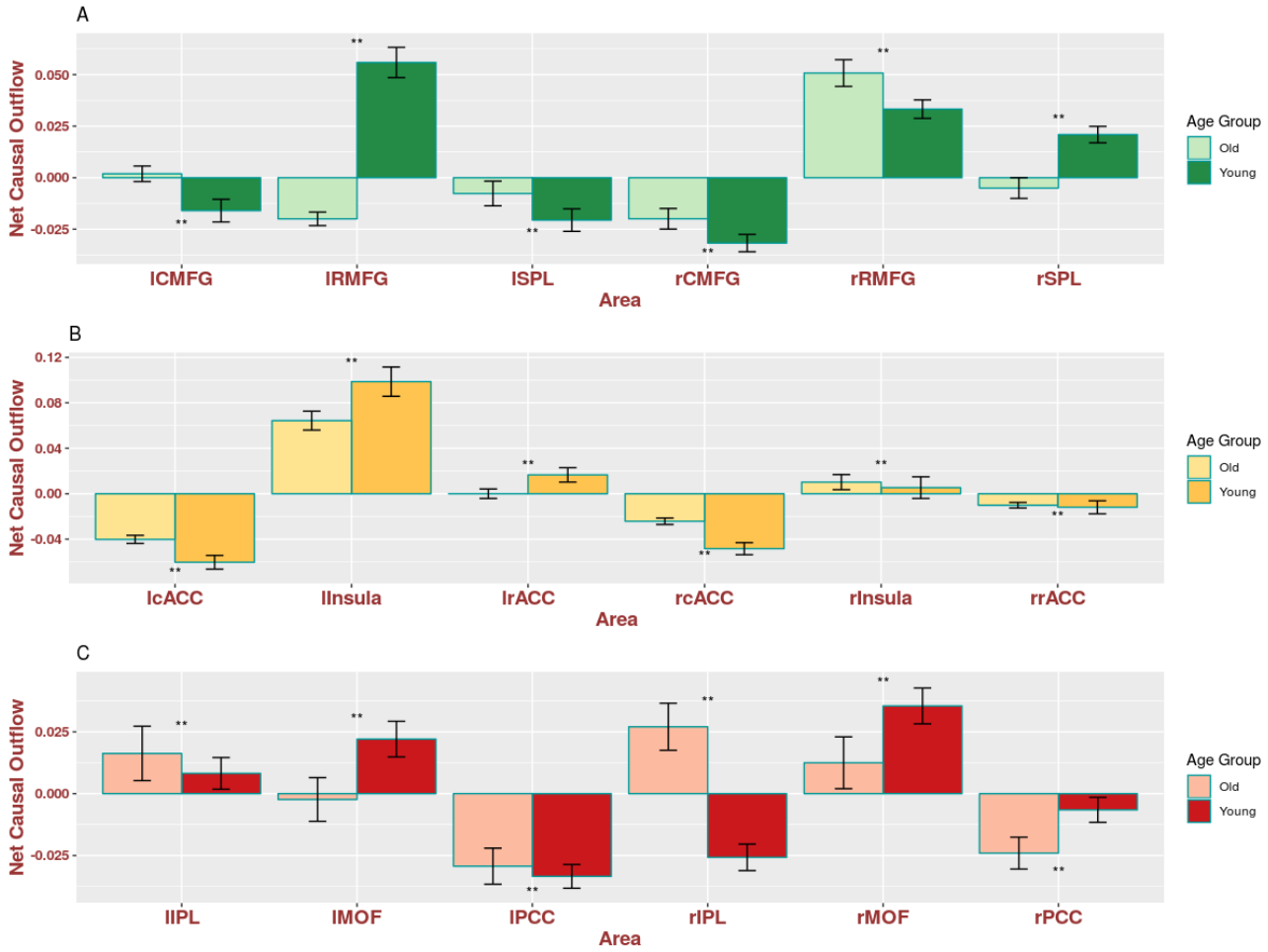
A
Net Causal Outflow
0.050
0.025
0.000
-0.025
ICMFG
IRMFG
ISPL
rCMFG
rRMFG
rSPL
Area
Age Group
Old
Young
B
Net Causal Outflow
0.12
0.08
0.04
0.00
-0.04
lcACC
lInsula
lrACC
rcACC
rInsula
rrACC
Area
Age Group
Old
Young
C
Net Causal Outflow
0.025
0.000
-0.025
IIPL
IMOF
IPCC
rIPL
rMOF
rPCC
Area
Age Group
Old
Young

Figure 4.

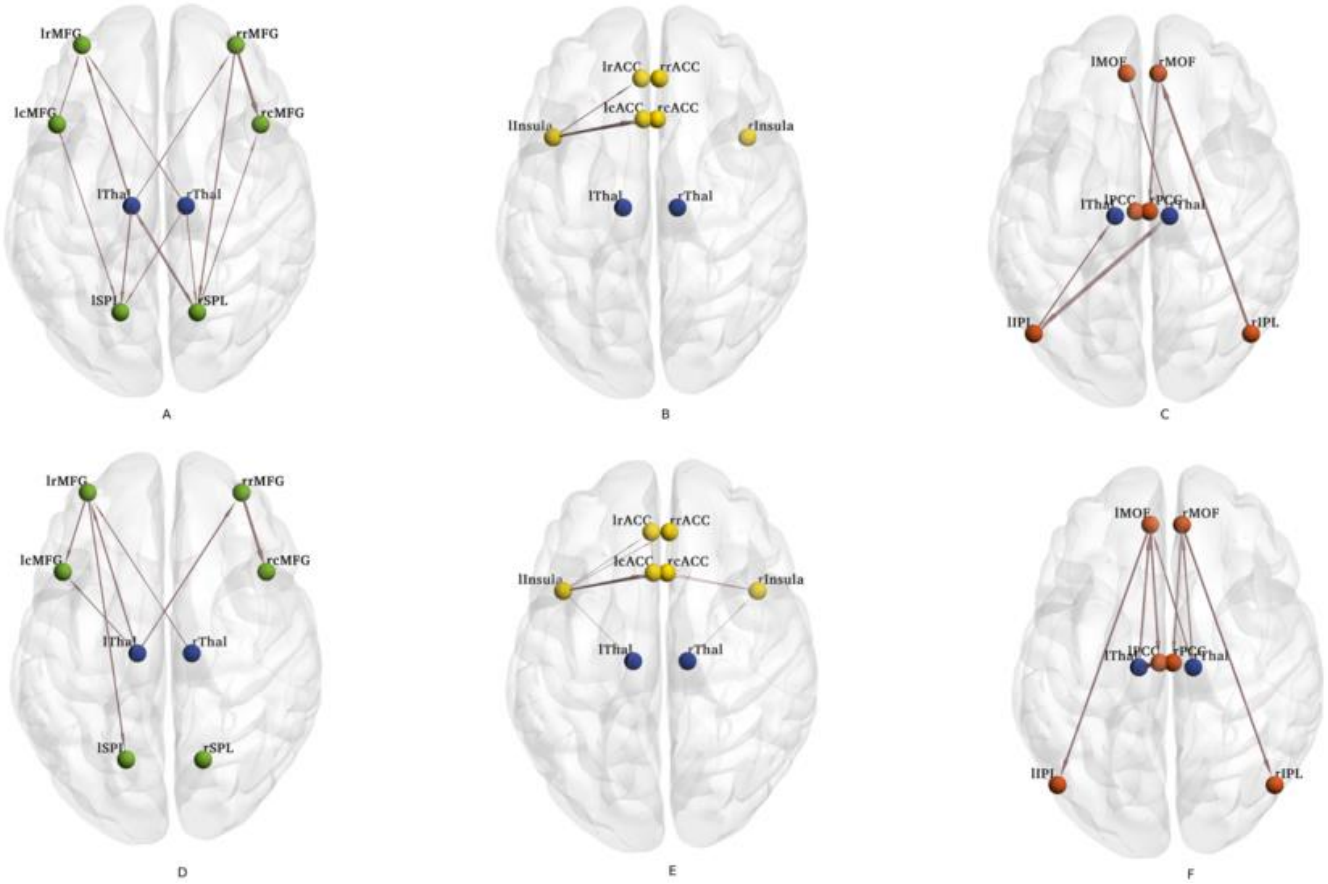
lrMFG
rrMFG
lcMFG
rcMFG
lThal
rThal
lSPL
rSPL
A
lrACC
rrACC
lcACC
rcACC
lInsula
rInsula
lThal
rThal
B
lMOF
rMOF
lPCC
rPCG
lThal
rThal
lIPL
rIPL
C
lrMFG
rrMFG
lcMFG
rcMFG
lThal
rThal
lSPL
rSPL
D
lrACC
rrACC
lcACC
rcACC
lInsula
rInsula
lThal
rThal
E
lMOF
rMOF
lPCC
rPCG
lThal
rThal
lIPL
rIPL
F

Figure 5.

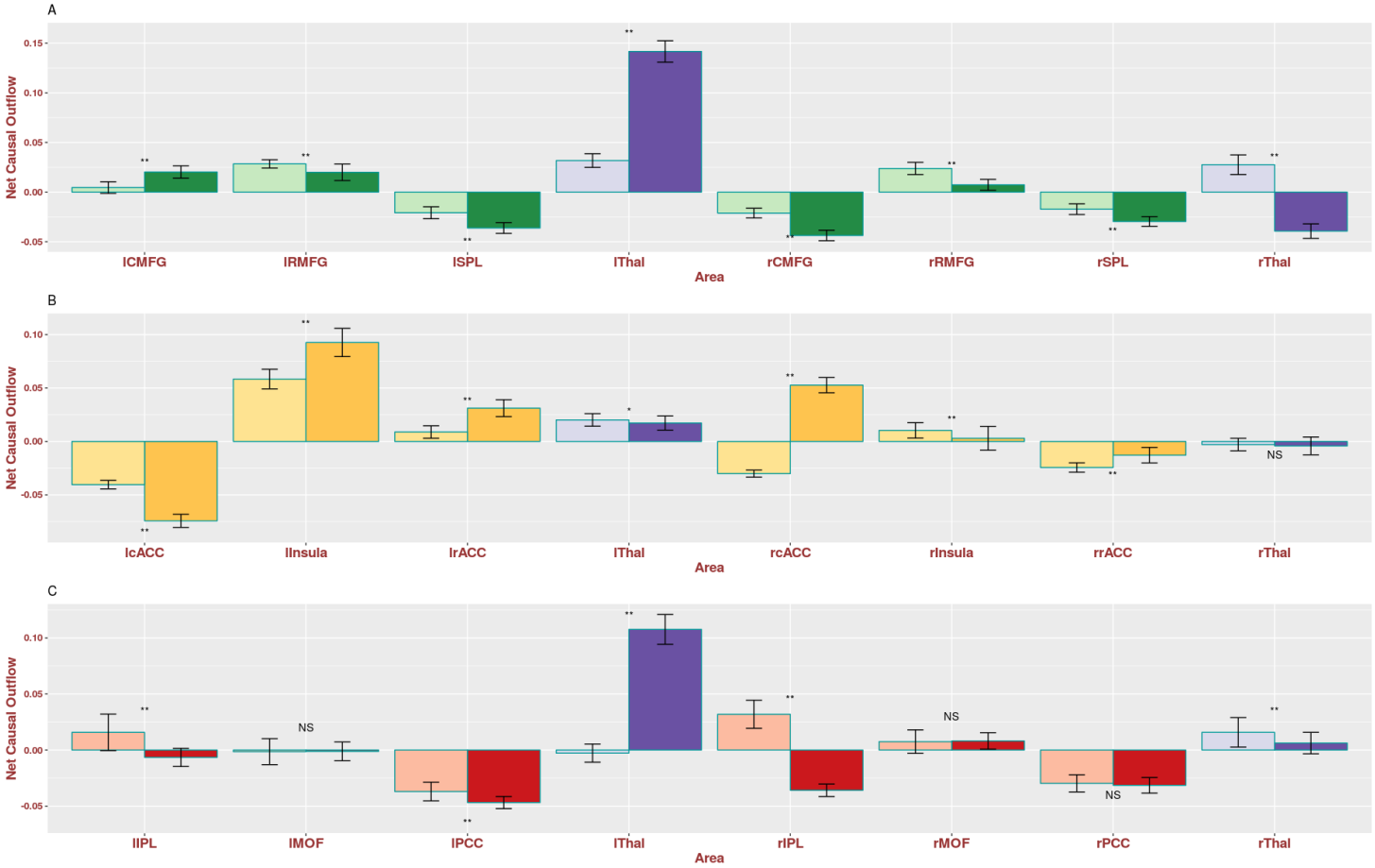
A
Net Causal Outflow
0.15
0.10
0.05
0.00
-0.05
lCMFG
lRMFG
lSPL
lThal
rCMFG
rRMFG
rSPL
rThal
Area
B
Net Causal Outflow
0.10
0.05
0.00
-0.05
lcACC
lInsula
lrACC
lThal
rcACC
rInsula
rrACC
rThal
NS
Area
C
Net Causal Outflow
0.10
0.05
0.00
-0.05
lIPL
lMOF
lPCC
lThal
rIPL
rMOF
rPCC
rThal
NS
Area

Figure 6.

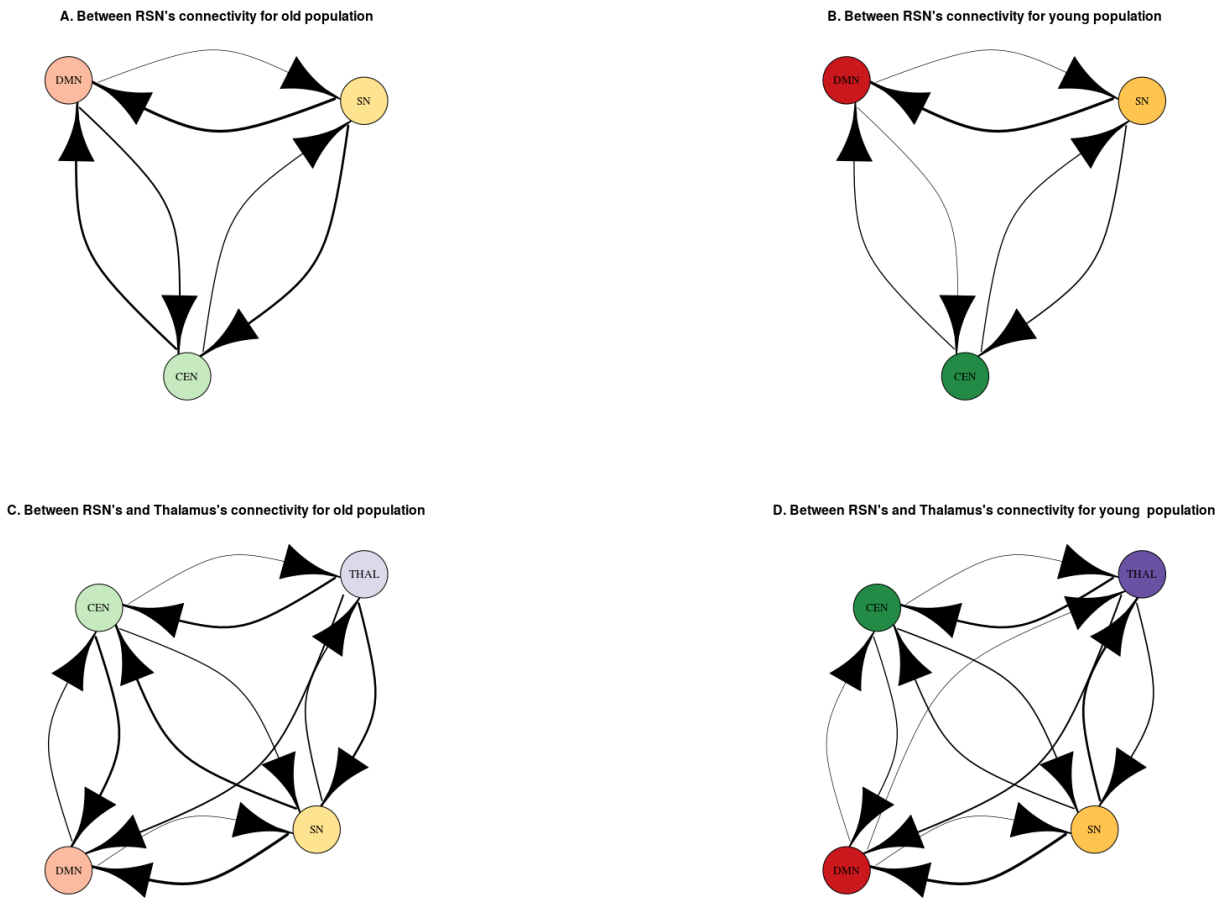
A. Between RSN's connectivity for old population
DMN
SN
CEN
B. Between RSN's connectivity for young population
DMN
SN
CEN
C. Between RSN's and Thalamus's connectivity for old population
CEN
THAL
SN
DMN
D. Between RSN's and Thalamus's connectivity for young population
CEN
THAL
SN
DMN

Figure 7.

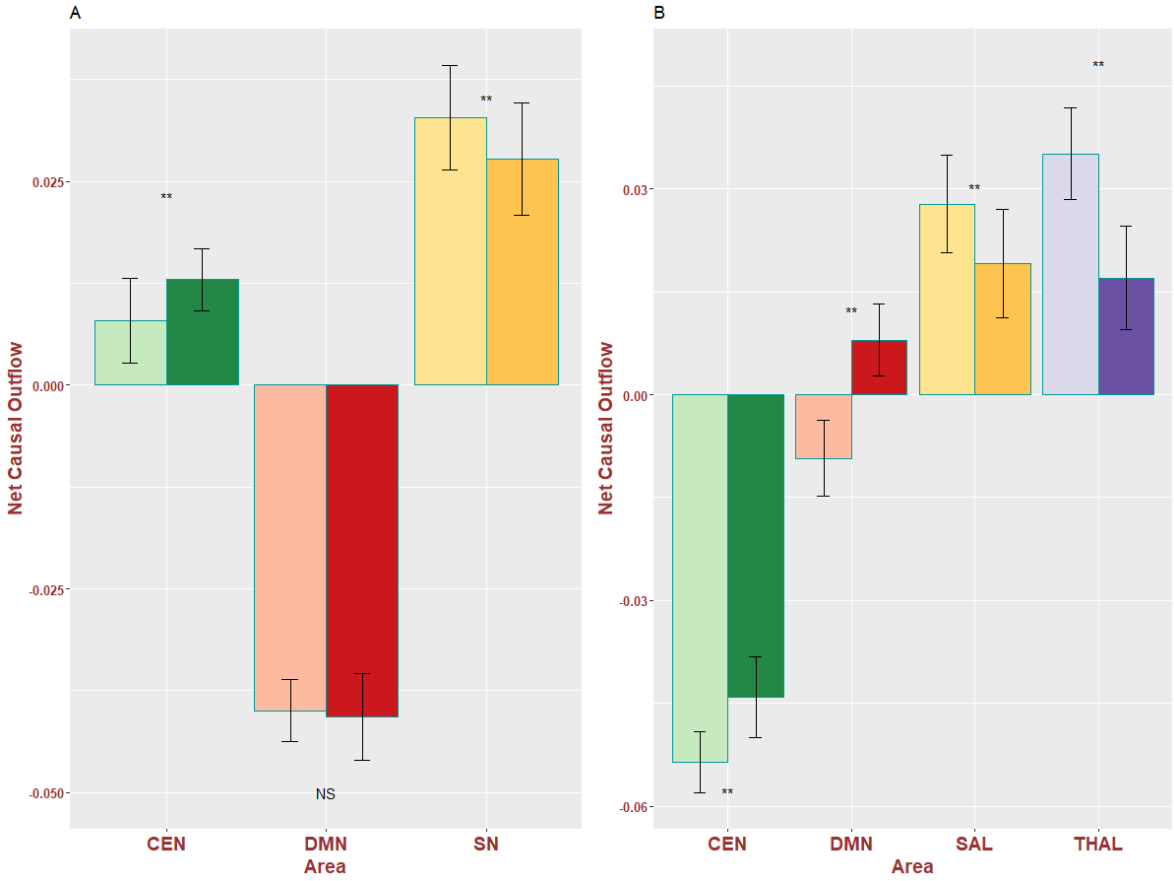
A
B
Net Causal Outflow
0.025
0.000
-0.025
-0.050
0.03
0.00
-0.03
-0.06
**
NS
CEN
DMN
SN
SAL
THAL
Area

Figure 8.

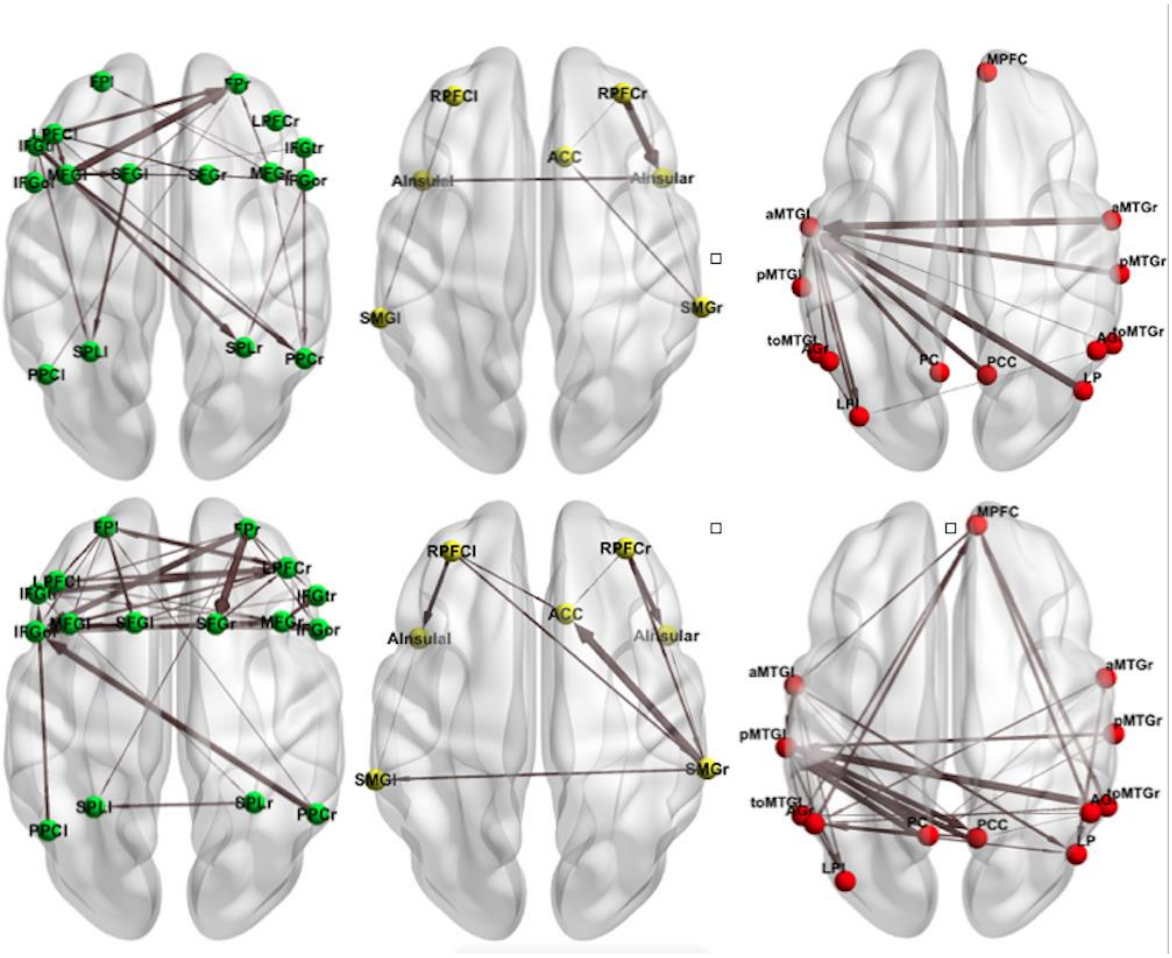
FPl
FPr
LPFCl
LPFCr
IFGtl
IFGtr
IFGol
MFGl
SFGl
SFGr
MFGr
IFGor
SPLl
SPLr
PPCl
PPCr
RPFCl
RPFCr
ACC
AInsular
SMGl
SMGr
MPFC
aMTGl
aMTGr
pMTGl
pMTGr
toMTGl
toMTGr
PC
PCC
LP
LPl

Figure 9.

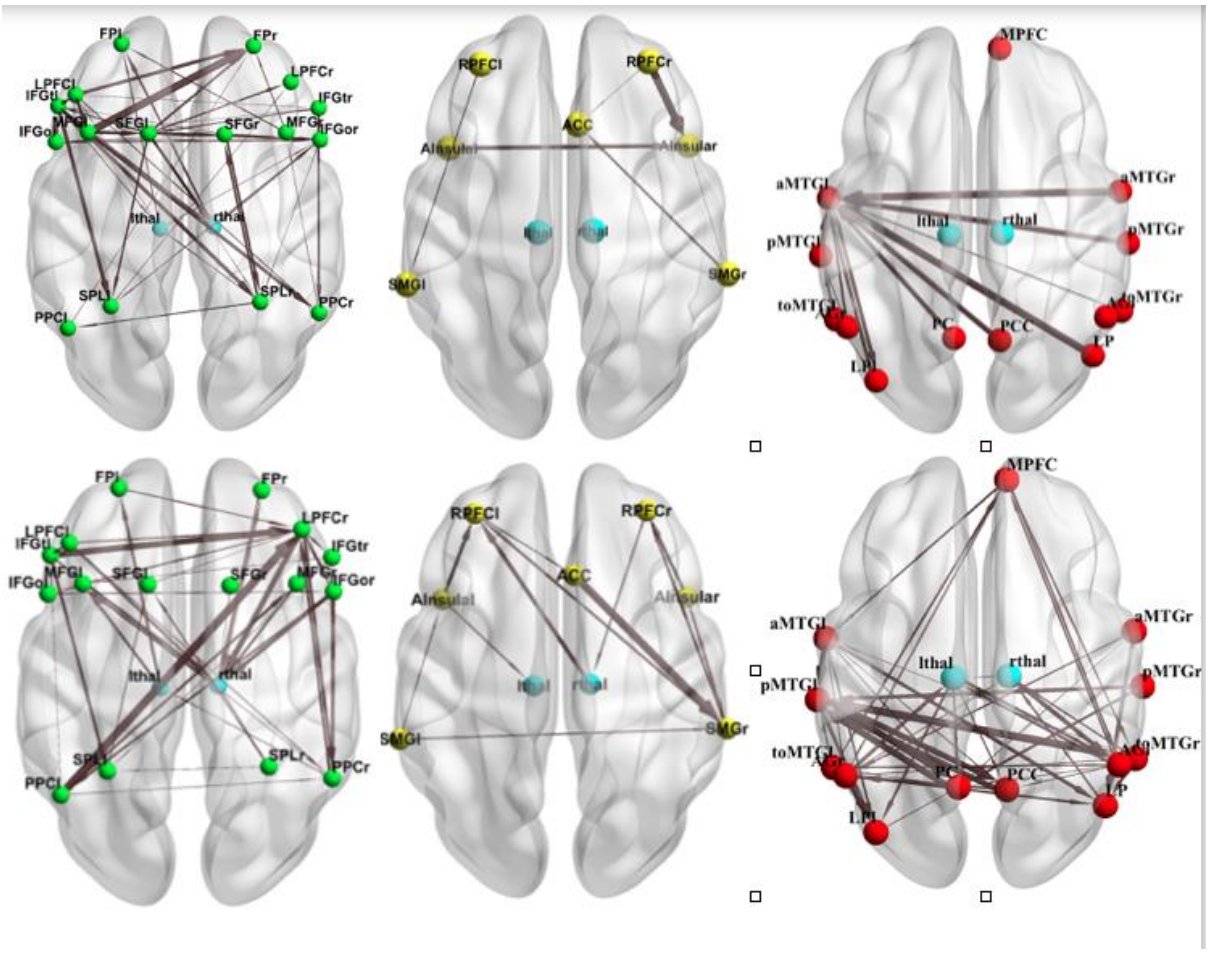
FPl
FPr
LPFCl
LPFCr
IFGtl
IFGtr
IFGol
IFGor
MFGl
SFGl
SFGr
MFGr
lthal
rthal
SPLl
SPLr
PPCl
PPCr
RPFCl
RPFCr
ACC
Alnsular
SMGl
SMGr
MPFC
aMTGl
aMTGr
pMTGl
pMTGr
toMTGl
toMTGr
PC
PCC
LP

Figure 10.